Electronic Supplementary information: Quantum and classical effects in DNA point mutations: Watson-Crick tautomerism in AT and GC base pairs

L. Slocombe,[a] J. S. Al-Khalili,[b] and M. Sacchi[c]

1 Additional Structures

In this section additional structures are shown. The monomeric structures are shown in Fig. 1 for A, Fig. 2 for T, G Fig. 3, and for C Fig. 4. The raw coordinates of the reactant, products, and transition states are available upon request.

2 Propagating the Schrödinger equation

For the spatial partial derivative in the Schrödinger equation we use the pseudo-spectral method, which is preferred over a finite difference approach due to its superior scaling when finer spatial grids are employed and it also improves numerical stability[1].

To propagate the wave packet in time, we use the DifferentialEquations.jl suite[2] which provides a comprehensive set of tools for solving ordinary differential equations. The numerical accuracy and time-stability of the wave packet scattering approach was benchmarked by comparing the numerically calculated, time-varying, expectation values to well known analytical solutions of a Gaussian sloshing in a harmonic well. A benchmark indicated that the ROCK4 algorithm[3], a fourth-order method based on the expansion of Chebyshev polynomials, offered a fair trade-off between speed and accuracy due to their stability properties.

The numerical parameters are summarised in Table 1.

Table 1 Summary of the numerical parameters used to obtain the tunnelling corrections in the Gaussian wave packet scattering approach.

Variable	Value	Description
n	2^{11}	Number of Fourier grid points
T	298.15 K	Temperature
m	1836 a.u.	Effective mass
tol	10^{-16}	Tolerance of adaptive time-stepping algorithm
σ	1.0 Å	Initial spatial width of wave packet
x_0	6.0 Å	Initial off-set of the wave packet

3 Additional Arrhenius plots

This section contains additional Arrhenius plots. See Fig. 5 for A-T. Whereas for the intrabase reactions see Fig. 6 for A, 7 T, 8 G, and 9 C respectively.

Notes and references

1 R. Kosloff, *Annu. Rev. Phys. Chem.*, 1994, **45**, 145–178.

2 C. Rackauckas and Q. Nie, *J. Open Res. Softw*, 2017, **5**, 15.

[a] *Leverhulme Quantum Biology Doctoral Training Centre, E-mail: l.slocombe@surrey.ac.uk*

[b] *Department of Physics,*

[c] *Department of Chemistry, University of Surrey, Guildford, GU2 7XH, UK. E-mail: m.sacchi@surrey.ac.uk*

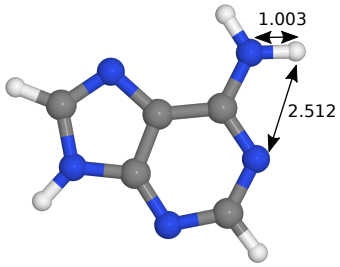

(a) Canonical structure of the Adenine monomer

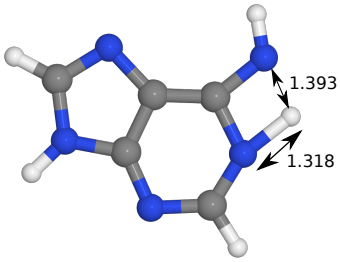

(b) Transition state for tautomerisation of Adenine

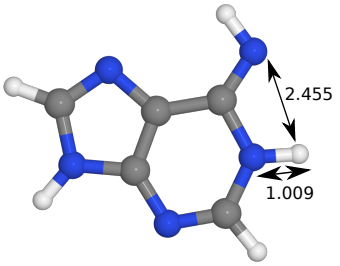

(c) Tautomeric structure of the Adenine

Fig. 1 Optimised geometries of the proton transfer reaction of Adenine, from the canonical to the tautomeric configuration. Lengths are reported in Å. For further information on the calculation details, see main text.

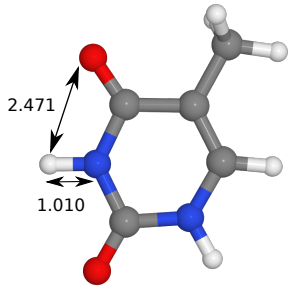

(a) Canonical structure of Thymine

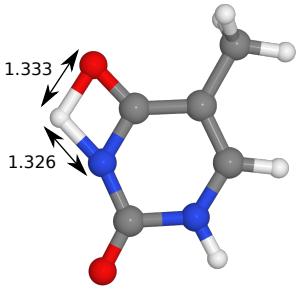

(b) Transition state for tautomerisation of Thymine

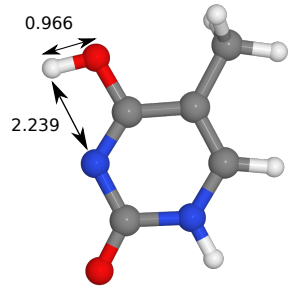

(c) Tautomeric structure of Thymine

Fig. 2 Optimised geometries of the proton transfer reaction of Thymine, from the canonical to the tautomeric configuration. Lengths are reported in Å. For further information on the calculation details, see main text.

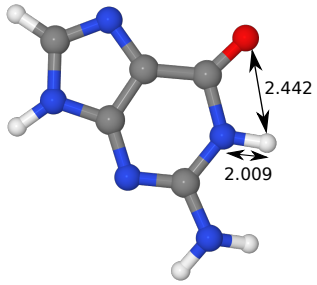

(a) Canonical Guanine

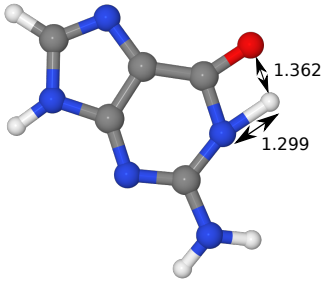

(b) Guanine transition state

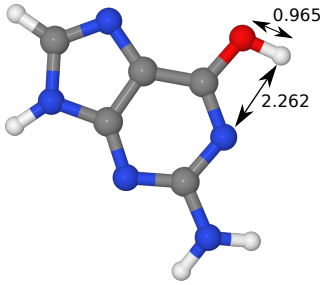

(c) Tautomeric Guanine

Fig. 3 Optimised geometries of the proton transfer reaction of Guanine, from the canonical to the tautomeric configuration. Lengths are reported in Å. For further information on the calculation details, see main text.

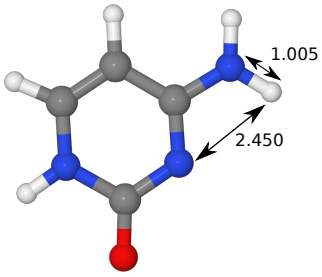

(a) Canonical Cytosine

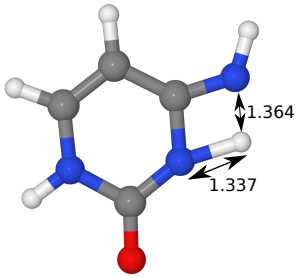

(b) Cytosine transition state

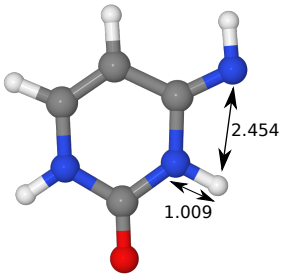

(c) Tautomeric Cytosine

Fig. 4 Optimised geometries of the proton transfer reaction of Cytosine, from the canonical to the tautomeric configuration. Lengths are reported in Å. For further information on the calculation details, see main text.

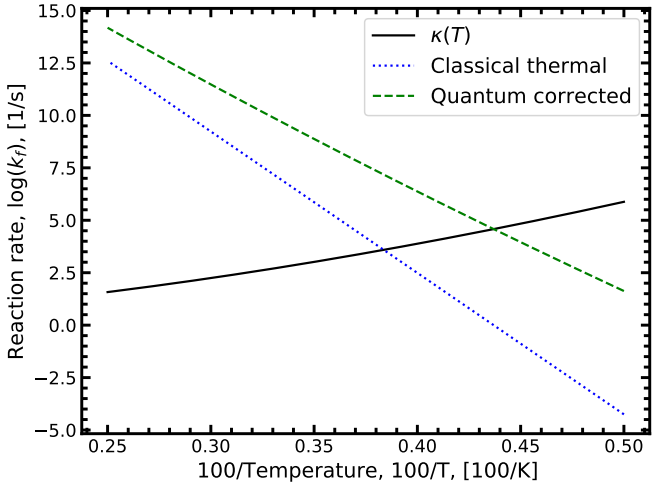

(a) A-T forward reaction rate

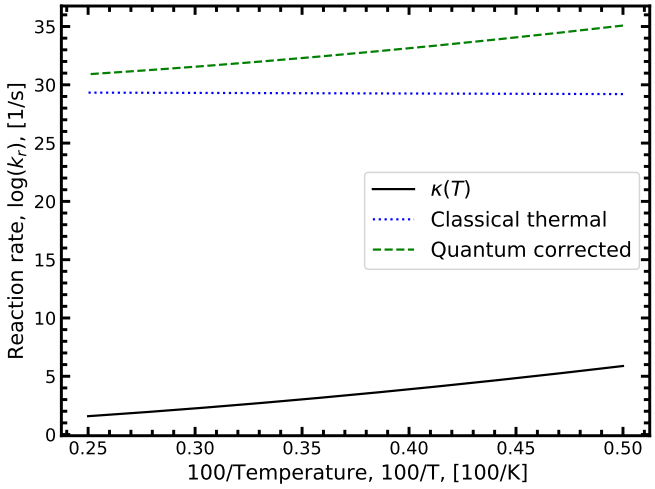

(b) A-T reverse reaction rate

Fig. 5 Arrhenius plot with quantum tunnelling corrections to the forward and reverse reaction rates for the double proton transfer of the Adenine–Thymine system. The transmission coefficient is evaluated using the Scattering approach.

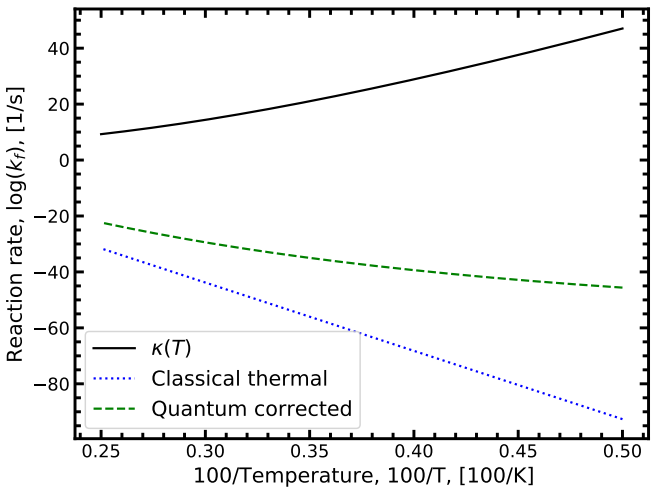

(a) A forward reaction rate

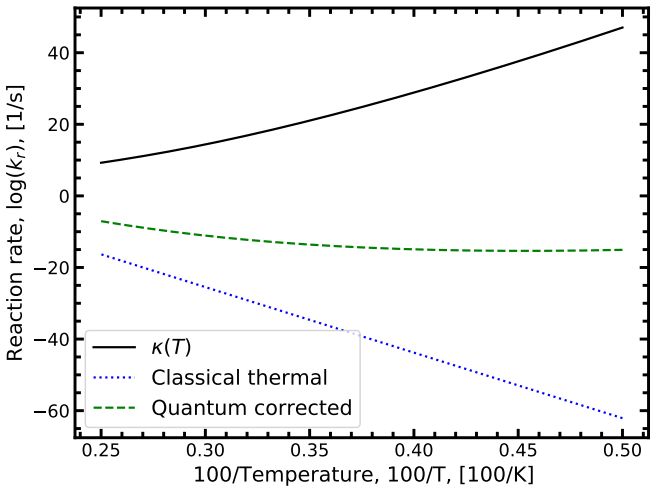

(b) A reverse reaction rate

Fig. 6 Arrhenius plot with quantum tunnelling corrections to the forward and reverse reaction rates for the double proton transfer of the Adenine system. The transmission coefficient is evaluated using the Scattering approach.

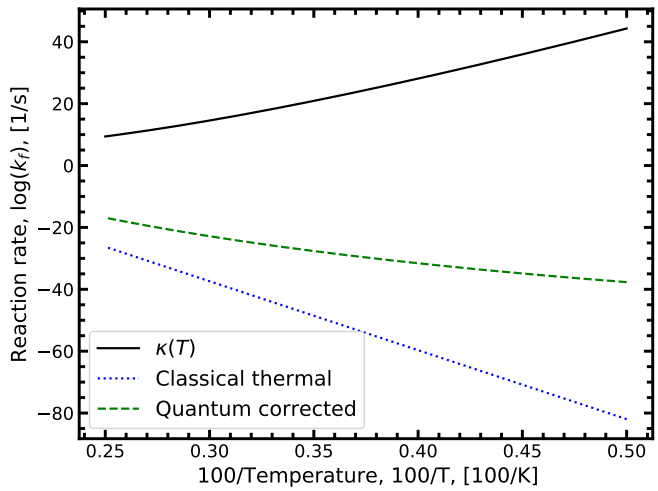

(a) T forward reaction rate

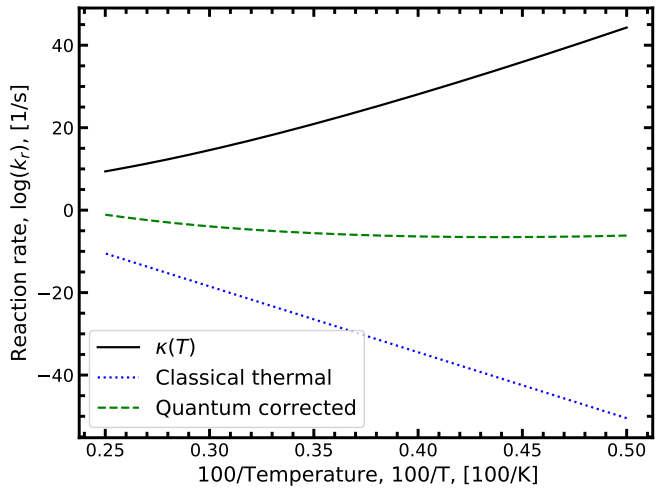

(b) T reverse reaction rate

Fig. 7 Arrhenius plot with quantum tunnelling corrections to the forward and reverse reaction rates for the double proton transfer of the Thymine system. The transmission coefficient is evaluated using the Scattering approach.

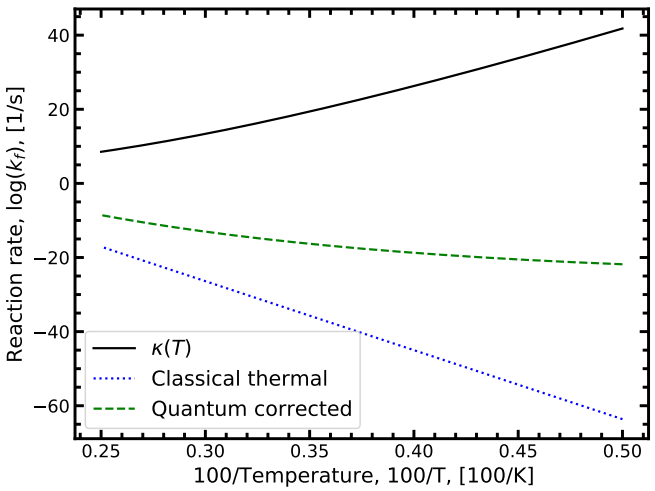

(a) G forward reaction rate

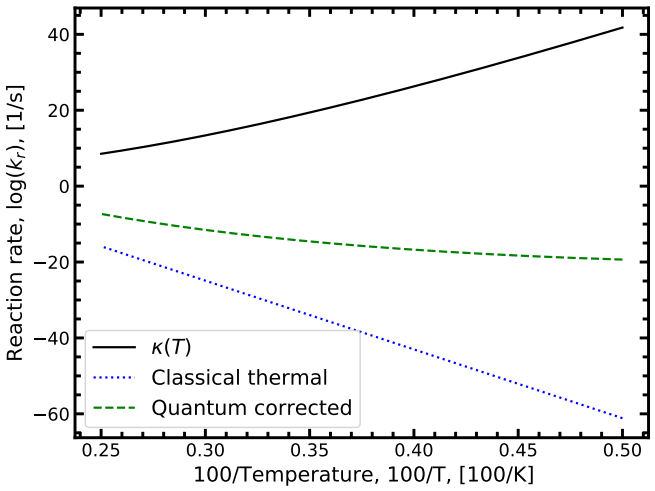

(b) G reverse reaction rate

Fig. 8 Arrhenius plot with quantum tunnelling corrections to the forward and reverse reaction rates for the double proton transfer of the Guanine system. The transmission coefficient is evaluated using the Scattering approach.

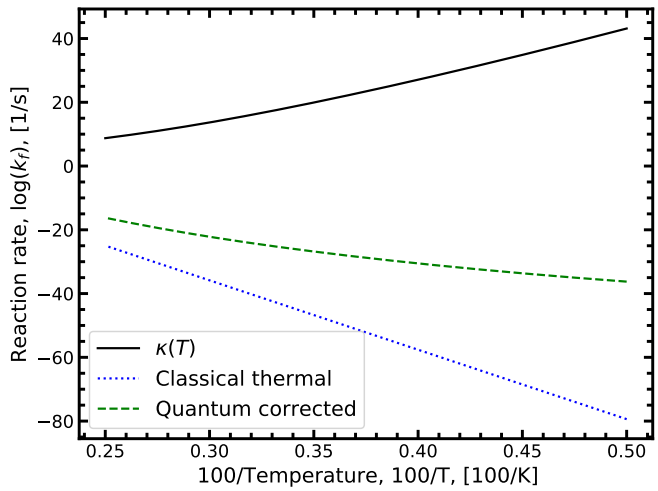

(a) C forward reaction rate

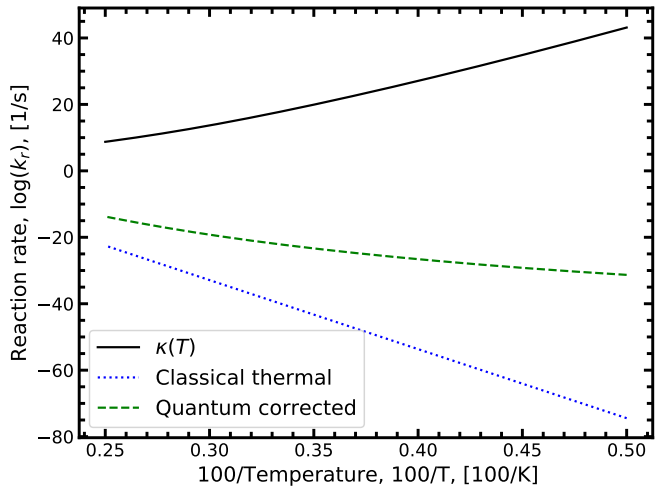

(b) C reverse reaction rate

Fig. 9 Arrhenius plot with quantum tunnelling corrections to the forward and reverse reaction rates for the double proton transfer of the Cytosine system. The transmission coefficient is evaluated using the Scattering approach.

3 A. Abdulle, *SIAM J. Sci. Comput.*, 2002, **23**, 2041–2054.